Supporting Information for "Agreement of CMIP5 simulated and observed ocean Anthropogenic CO$_2$ uptake"

1. Estimates of ocean anthropogenic carbon

1.1. ΔC^*

The so-called ΔC^*-method [*Gruber et al.*, 1996] for estimating C_{ant} consists of measuring total DIC in the ocean and subsequently estimating the background carbon to separate the anthropogenic component. The ΔC^*-method has associated uncertainties, in addition to errors inherent to discrete observations. Firstly, the calculation assumes a constant disequilibrium between the oceanic and atmospheric pCO$_2$, which leads to overestimation of C_{ant} in the upper thermocline and underestimation of C_{ant} in the deep ocean [*Matsumoto and Gruber*, 2005]. Other errors include a young water age bias due to the CFC-based method [*Haine and Hall*, 2002], which affects the time at which water parcels were exposed to atmospheric pCO$_2$ levels. Lastly, the method implicitly assumes that C_{ant} transport is advective only. *Matsumoto and Gruber* [2005] provided a test of these assumptions by applying the ΔC^*-method to a "true" distribution of C_{ant} from a coupled climate model. They found that C_{ant} is underestimated in older waters, and overestimated in younger waters. They found that C_{ant} inventories estimated by ΔC^*-method are biased upwards by 7%, which is within the quoted uncertainty of the method. However, the method also assumes constant Redfield ratios, which holds globally but has been shown to vary spatially [*Weber and Deutsch*, 2010]. The resulting error from this assumption is uncertain.

1.2. Greens function

Khatiwala et al. [2009] presented an observation-based Green's function method similar to *Waugh et al.* [2006], which is a generalized form of the transit tracer method as employed by *Waugh et al.* [2006]. It is based on constructing an estimate of ocean transport based on observations of ocean tracers: CFC-11, CFC-12, natural ^{14}C, salinity, temperature, and PO$_4^*$. For the surface flux of carbon, it is assumed that atmosphere-ocean disequilibrium scales linearly with the atmospheric pCO$_2$ perturbation. The method is therefore entirely observation-based. To test the method, *Khatiwala et al.* [2009] applied it to a "truth" constructed from an ocean-only simulation and note a 2% error in the direct comparison. One caveat that applies to both of the observational estimates discussed above is they do not include the effects of changes in circulation and temperature, whereas the C_{ant} from model simulations generally does. Unlike the ΔC^*-method method however, the Green's function method does include biogeochemical changes.

1.3. Model simulations

CMIP5 ESM historical model simulations are used to assess simulated ocean carbon uptake are those from ESMs. In these experiments, atmospheric pCO$_2$ levels are pre-scribed from 1850 to 2005. Prescribing atmospheric pCO$_2$ rather than carbon emissions provides a tighter constraint on the

simulation and isolates differences in ocean carbon uptake, since all the ocean models are exposed to the same atmospheric pCO$_2$ values. In the CMIP5 historical simulations, C$_{ant}$ is simply taken as the difference in DIC over the historical period with the pre-industrial control simulation. It therefore includes changes in natural carbon (the background distribution of carbon that is not due to atmospheric anomalies) as well as the anthropogenic carbon perturbation. To quantify the effect of climate change on the oceanic natural carbon reservoir, some ESMs ran simulations calculating only the change in natural carbon over both the historical period and in an idealized scenario whereby atmospheric CO$_2$ levels increase by 1% every year as part of CMIP5, similar to studies by *Plattner et al.* [2001], *Keeling* [2005], *Wang et al.* [2012], and *McNeil and Matear* [2013]. The average of the CMIP5 simulations, at a time when atmospheric pCO$_2$ is at year 1995 levels, is a 3 $\pm$ 3.9 Pg C change in natural carbon. Because the underlying assumptions made by the observational estimates are generally similar, they do not explain the large difference in their best estimates. The difference between the models and the observations due to "natural" carbon changes are also not likely to be large enough to explain the large negative bias of the CMIP5 model C$_{ant}$.

2. Impulse response functions

To provide a second estimate of $\Delta C_{1791-1850}$ and $\Delta C_{1765-1791}$ for verification, we use the impulse response functions (IRFs) from *Joos et al.* [2013]. To use the impulse response functions, we need to know what the effective carbon emissions are from 1765 up to 1995, due to both land use changes and fossil fuel emissions. Land emissions are very uncertain prior to 1850 and have previously been estimated in *Khatiwala et al.* [2009] as the difference between fossil fuel emissions and the combined ocean carbon and atmospheric carbon content. For this study, we use the atmospheric impulse response function and measured atmospheric pCO$_2$ history to recursively calculate the required yearly carbon emissions at year t, $E(t)$, to produce the measured pCO$_2^{atm}$ values:

$$E(t) = 2.13. * pCO_2^{atm}(t) - \sum_{t_0}^{t-1} I(t-\tau)E(\tau)d\tau, \qquad (1)$$

where t_0 is the start date of the adjustment and the constant 2.13 converts parts per million in the atmosphere to Pg C [*Clark*, 1982]. The choice of IRFs affects the total emissions required to produce the measured pCO$_2^{atm}$ values. To calculate the time evolution of $\Delta C_{1791-1850}$ we repeat the procedure outlined in the paragraph above but set atmospheric pCO$_2$ after 1850 constant at the 1850 value (286.4 ppm), and similarly for $\Delta C_{1765-1791}$. To maintain a set atmospheric pCO$_2$, additional emissions are required as the ocean and land continue to absorb atmospheric carbon. Figure 1 shows the implied emissions that drive $\Delta C_{1765-1791}$ and $\Delta C_{1791-1850}$, $E_{1765-1791}$ and $E_{1791-1850}$ respectively, as well as the emissions for the *Joos et al.*

[2013] experiments and observations of fossil fuel emissions [*Houghton*, 2003; *Boden et al.*, 2009]. Over the historical period, changes in ocean carbon chemistry and circulation affect the rate of ocean carbon uptake. Ocean carbon uptake therefore responds non-linearly to emissions. As a result, the IRFs for the early industrial ocean are different than those for present-day conditions, as illustrated by *Joos et al.* [2013]. Our linear IRF-based adjustment is supported by 1) the smallness of the adjustment-implied emissions relative to the total emissions over the same period and 2) the time and magnitude of the adjustments are close to those of the pulse emission used to calibrate the IRFs that we use.

3. Ocean carbon uptake after atmospheric $p\mathrm{CO_2}$ stabilization

In this section, we discuss the uptake of ocean carbon after atmospheric CO_2 has stabilized, following on from section 4 in the main text. The results from the main text show that the majority of $\Delta C_{1765-1791}$ and $\Delta C_{1791-1850}$ is absorbed after 1791 and 1850 respectively, after atmospheric $p\mathrm{CO_2}$ levels stabilized. The CMIP5 simulations begin from an equilibrated year 1850 state. The surface carbon concentrations in this equilibrated state will not be the same as a transient system with the same atmospheric $p\mathrm{CO_2}$ which has experienced a complete $p\mathrm{CO_2}$ history. This concept can be demonstrated by utilizing the TMM simulations to calculate $\Delta C_{1765-1791}$, in which atmospheric $p\mathrm{CO_2}$ is increased from 1765 to 1791 and then kept constant.

In these experiments, the surface DIC at the time of atmospheric $p\mathrm{CO_2}$ stabilization is less than it would be at equilibrium for the same atmospheric $p\mathrm{CO_2}$ value. This is illustrated in Fig. 2A , where the surface DIC anomaly at the end of the experiment, when the system is more equilibrated like the CMIP5 models, is higher then at the start of the atmospheric $p\mathrm{CO_2}$ stabilization. At both points in time, the atmospheric $p\mathrm{CO_2}$ is the same but the surface carbon concentration is different. The pale blue region in panel A then represents the air-sea disequilibrium of surface DIC, DIC_{diseq}, which decreases with time. Figure 2B then shows the evolution of ocean anthropogenic carbon. After atmospheric $p\mathrm{CO_2}$ has stabilized, ocean anthropogenic carbon continues to increase since the surface DIC has not equilibrated. The pale blue region in panel B, $C_{ant\ diseq}$ represents the carbon uptake that results from the air-sea disequilibrium DIC_{diseq} after atmospheric $p\mathrm{CO_2}$ has stabilized.

4. Constant IRF assumption

The IRFs from *Joos et al.* [2013] are calculated with respect to an 1850-equilibrated ocean, so the effective Revelle Buffer Factor R is that of an 1850 ocean. However, the adjustments made in the main text begin in 1765 at which time the buffer factor was likely less than it was in 1850, while post-1850, the buffer factor would have been larger. In effect, using the IRFs biases our adjustments too low before 1850 and too high after 1850. To calculate the error this introduces, we use the framework developed by *Goodwin et al.* [2007]. In that framework, we make the assumption that the buffered carbon inventory I_B remains constant, which is shown in *Goodwin et al.* [2007] to hold well for total emissions of carbon up to 5000 Pg C, and using the following equation:

$$I_B = I_A + \frac{I_O}{R}, \tag{2}$$

where I_A and I_O are the atmospheric and oceanic carbon inventories respectively. Using eqn. 2 and the time evolution of ocean and atmospheric carbon from *Khatiwala et al.* [2009], we can calculate the likely value of R. Figure 3A shows the changes in the buffer factor induced by the total adjustment in ocean carbon from the changes in atmospheric $p\mathrm{CO_2}$ between 1765 to 1850, in blue, and the implied changes in ocean buffer factor due to the changes in atmospheric $p\mathrm{CO_2}$ after 1850, in red. Figure 3B shows the net resulting estimated percentage error that we get by using IRFs referenced to 1850, by assuming the ocean uptake is directly proportional to the buffer factor. The 4.5% uncertainty in 1995 that results from this calculation is less than our claimed error in the adjustments.

It is also worth noting that while the effect of the Buffer Factor, R, may be small, there is also the possibility that the ratio between the background ocean $p\mathrm{CO_2}$ (equal to atmospheric $p\mathrm{CO_2}$) and the background mixed layer dissolved inorganic carbon, DIC, content might change due the non-linearity of ocean chemistry. This is relevant for the buffer factor relationship which dictates the change in surface ocean $p\mathrm{CO_2}$, $\Delta p\mathrm{CO_2}$, given a change in ocean DIC, ΔDIC, i.e.:

$$\frac{\Delta pCO_2}{pCO_2} = R\frac{\Delta DIC}{DIC} \tag{3}$$

For the adjustments that are made in the main text, the change in ocean carbon is around 30 Pg (due to the 1765-1850 change in atmospheric $p\mathrm{CO_2}$), and the change in atmospheric $p\mathrm{CO_2}$ is around 10 ppm. The surface ocean contains around 900 Pg C, so a 30 Pg C perturbation constitutes around 3.3%. Similarly, a 10 ppm perturbation on a 280 ppm background is a 3.5% perturbation. The change in ratio DIC/pCO_2 is therefore virtually constant over the range of emissions due to the adjustments to ocean carbon we are making.

5. Individual model bias

In the main text, the ensemble mean bias of the CMIP5 model anthropogenic carbon uptake is compared to the observations. However, there is some variation in the bias between the individual models. Figure 4 shows the column integrated 1995 anthropogenic carbon bias of the CMIP5 models relative to the adjusted observational mean. Most models show the behavior discussed in the main text: a positive bias in the Southern Indian and Pacific Oceans, and a negative bias in the Southern Ocean. However, some models do not obviously exhibit this bias, namely CNRM, the GFDL models and to some extent GISS-E2-R-CC. However, these models show a maximum in Southern Ocean wind stress more poleward than the CMIP5 mean so are more similar to the real world which may mean that the biases plotted are due to other factors. The dipole bias discussed in the main text is therefore not a result of a few outliers, but indicative of the CMIP5 models as a set.

6. Model drift

When calculating the anthropogenic carbon in the CMIP5 models, the ocean carbon from the historical simulation is subtracted from the tandem pre-industrial control simulation. However, the degree of equilibration of the control simulation varies between the models. Figure 5 shows a scatter plot of the drift in oceanic carbon between 1860

and 1995 in the control simulation against the total anthropogenic carbon storage over the same period. Some models show significant drift over the historical period, up to -122 Pg C. However, we believe that there is no causal relationship between drift and anthropogenic carbon storage, similar to findings by *Frölicher et al.* [2015], even though the correlation coefficient between drift and C_{ant} storage is -0.63, since the correlation depends on a few outliers. Nonetheless, the focus of this study is the ensemble mean bias, and the mean drift of the ensemble is close to zero.

References

References

Boden, T. A., G. Marland, and R. J. Andreas (2009), Global, Regional, and National Fossil-fuel CO2 Emissions, *Carbon Dioxide Information Analysis Center, Oak Ridge National Laboratory, 2009)*, doi:10.3334/CDIAC/00001 (.

Clark, W. C. e. (1982), Carbon Dioxide Review: 1982, *Oxford University Press, New York*.

Frölicher, T. L., J. L. Sarmiento, D. J. Paynter, J. P. Dunne, J. P. Krasting, and M. Winton (2015), Dominance of the Southern Ocean in Anthropogenic Carbon and Heat Uptake in CMIP5 Models, *Journal Of Climate*, *28*(2), 862–886, doi:10.1175/JCLI-D-14-00117.1.

Goodwin, P., R. G. Williams, M. Follows, and S. Dutkiewicz (2007), Ocean-atmosphere partitioning of anthropogenic carbon dioxide on centennial timescales, *Global Biogeochemical Cycles*.

Gruber, N., J. Sarmiento, and T. Stocker (1996), An improved method for detecting anthropogenic CO2 in the oceans, *Global Biogeochemical Cycles*, *10*(4), 809–837, doi:10.1029/96GB01608.

Haine, T., and T. Hall (2002), A generalized transport theory: Water-mass composition and age, *Journal Of Physical Oceanography*, *32*(6), 1932–1946, doi:10.1175/1520-0485(2002)032¡1932:AGTTWM¿2.0.CO;2.

Houghton, R. (2003), Revised estimates of the annual net flux of carbon to the atmosphere from changes in land use and land management 1850-2000, *Tellus Series B-Chemical And Physical Meteorology*, *55*(2), 378–390, doi:10.1034/j.1600-0889.2003.01450.x, 6th International Carbon Dioxide Conference, Sendai, Japan, Oct 01-05, 2001.

Joos, F., R. Roth, J. S. Fuglestvedt, G. P. Peters, I. G. Enting, W. von Bloh, V. Brovkin, E. J. Burke, M. Eby, N. R. Edwards, T. Friedrich, T. L. Froelicher, P. R. Halloran, P. B.

Holden, C. Jones, T. Kleinen, F. T. Mackenzie, K. Matsumoto, M. Meinshausen, G. K. Plattner, A. Reisinger, J. Segschneider, G. Shaffer, M. Steinacher, K. Strassmann, K. Tanaka, A. Timmermann, and A. J. Weaver (2013), Carbon dioxide and climate impulse response functions for the computation of greenhouse gas metrics: a multi-model analysis, *Atmospheric Chemistry And Physics*, *13*(5), 2793–2825, doi:10.5194/acp-13-2793-2013.

Keeling, R. (2005), Comment on "The ocean sink for anthropogenic CO₂", *Science*, *308*(5729), doi:10.1126/science.1109620.

Khatiwala, S., F. Primeau, and T. Hall (2009), Reconstruction of the history of anthropogenic co2 concentrations in the ocean, *Nature*, *462*.

Matsumoto, K., and N. Gruber (2005), How accurate is the estimation of anthropogenic carbon in the ocean? An evaluation of the Delta C* method, *Global Biogeochemical Cycles*, *19*(3), doi:10.1029/2004GB002397.

McNeil, B. I., and R. J. Matear (2013), The non-steady state oceanic CO₂ signal: its importance, magnitude and a novel way to detect it, *Biogeosciences*, *10*(4), 2219–2228, doi:10.5194/bg-10-2219-2013.

Plattner, G., F. Joos, T. Stocker, and O. Marchal (2001), Feedback mechanisms and sensitivities of ocean carbon uptake under global warming, *Tellus Series B-Chemical And Physical Meteorology*, *53*(5), 564–592, doi:10.1034/j.1600-0889.2001.530504.x.

Sabine, C., R. Feely, N. Gruber, R. Key, K. Lee, J. Bullister, R. Wanninkhof, C. Wong, D. Wallace, B. Tilbrook, F. Millero, T. Peng, A. Kozyr, T. Ono, and A. Rios (2004), The oceanic sink for anthropogenic CO2, *Science*, *305*(5682), 367–371, doi:10.1126/science.1097403.

Wang, S., J. K. Moore, F. W. Primeau, and S. Khatiwala (2012), Simulation of anthropogenic CO2 uptake in the CCSM3.1 ocean circulation-biogeochemical model: comparison with data-based estimates, *Biogeosciences*, *9*(4), 1321–1336, doi:10.5194/bg-9-1321-2012.

Waugh, D. W., T. M. Hall, B. I. McNeil, R. Key, and R. J. Matear (2006), Anthropogenic CO2 in the oceans estimated using transit time distributions, *Tellus Series B-Chemical And Physical Meteorology*, *58*(5), 376–389, doi:10.1111/j.1600-0889.2006.00222.x, 7th International Carbon Dioxide Conference (CO2), Boulder, CO, SEP 25-30, 2005.

Weber, T., and C. Deutsch (2010), Ocean nutrient ratios governed by plankton biogeography, *Nature*, *467*.
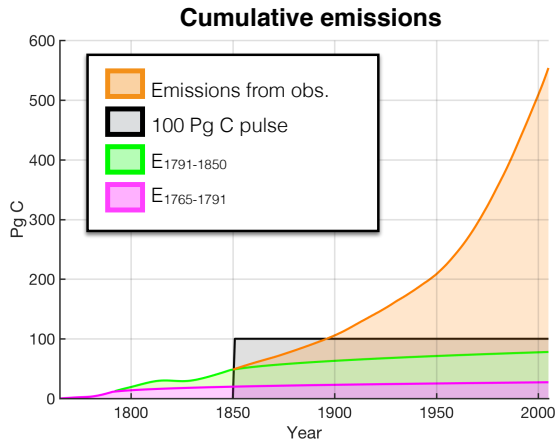
Figure 1. Cumulative emissions of carbon due to fossil fuel emissions from *Boden et al.* [2009] and *Houghton* [2003] between 1850-2005 (orange), the 100 Pg C pulse emission from *Joos et al.* [2013] (black), and the implied emissions for the adjustments due to the additional atmospheric pCO$_2$ forcing for *Sabine et al.* [2004] and *Khatiwala et al.* [2009] (green and magenta, respectively). The implied emissions for the adjustments are calculated using the pre-industrial IRFs from *Joos et al.* [2013] .
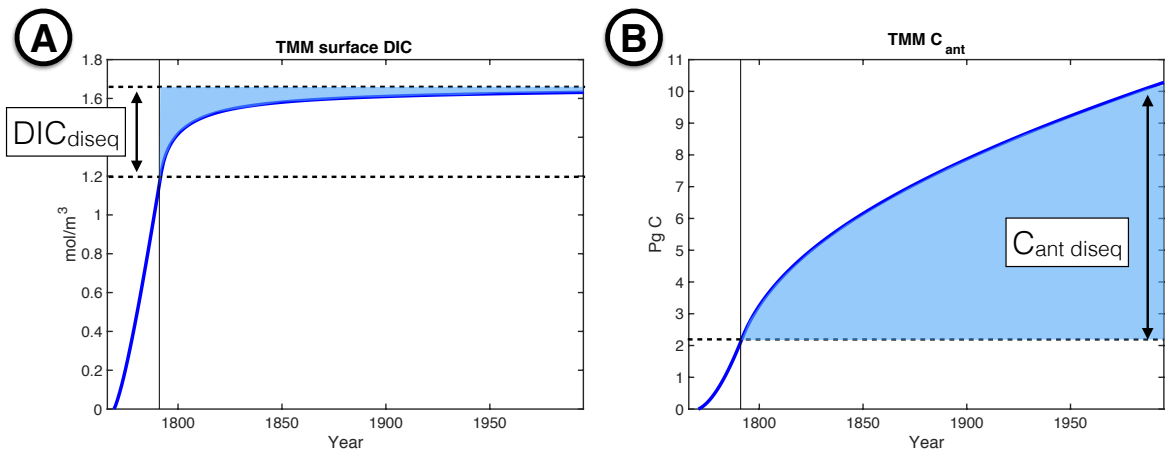
Figure 2. A) global mean surface DIC anomaly and B) global ocean carbon uptake for $\Delta C_{1765-1791}$. The vertical black lines show the time at which atmospheric pCO$_2$ stabilizes and is constant afterwards. The pale blue region in panel A represent the air-sea disequilibrium in surface DIC and the pale blue region represents the ocean carbon uptake associated with the that surface DIC disequilibrium.
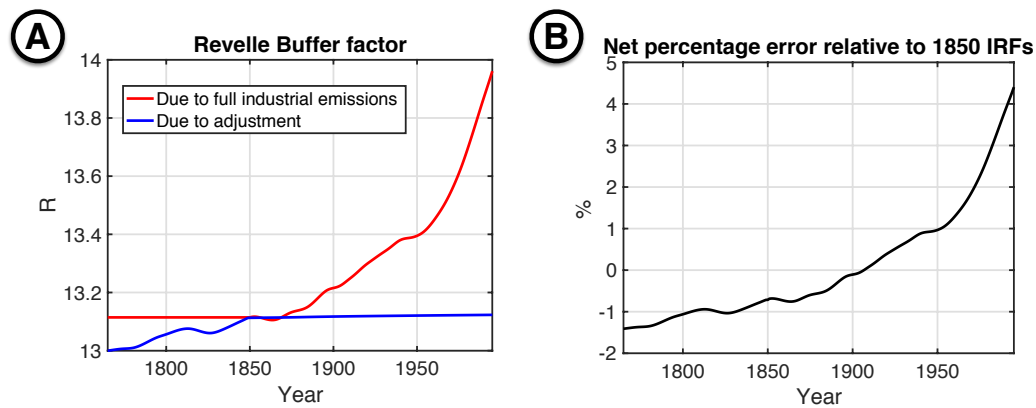
Figure 3. A) Time evolution of the global mean Revelle buffer factor induced by the adjustment in ocean carbon from the changes in atmospheric $p\mathrm{CO}_2$ between 1765 to 1850, in blue, and the implied changes in Revelle buffer factor due to the changes in atmospheric $p\mathrm{CO}_2$ after 1850, in red. B) The net resulting estimated percentage error in ocean anthropogenic carbon uptake calculated with IRFs, due to assuming a constant Revelle Buffer Factor.
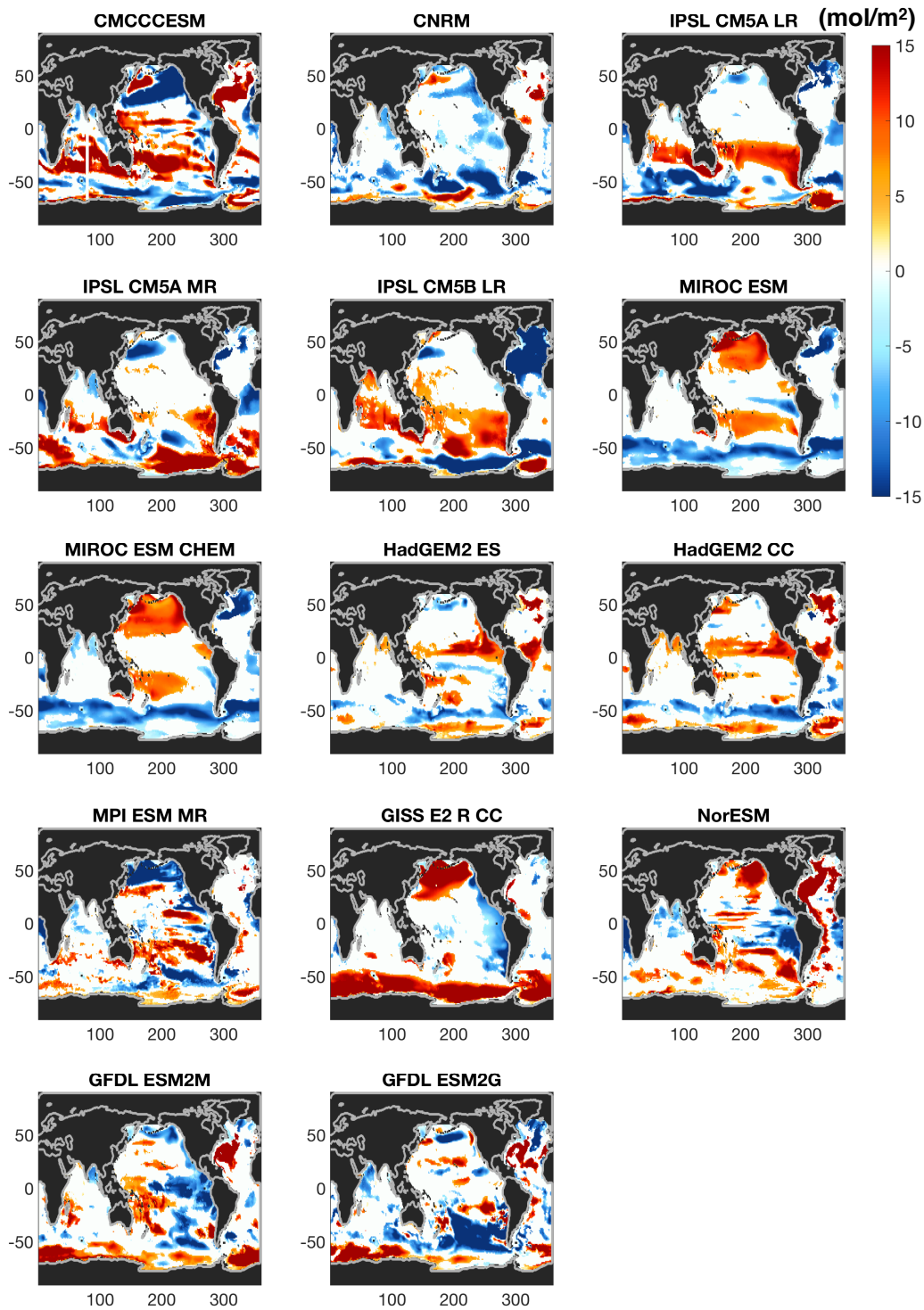
Figure 4. Individual CMIP5 model bias of column-integrated 1995 anthropogenic carbon relative to the mean of the adjusted *Khatiwala et al.* [2009] *Sabine et al.* [2004] estimates. The white areas are where the bias is less than the error in the observations, and the dark grey areas are those not covered by the observations.
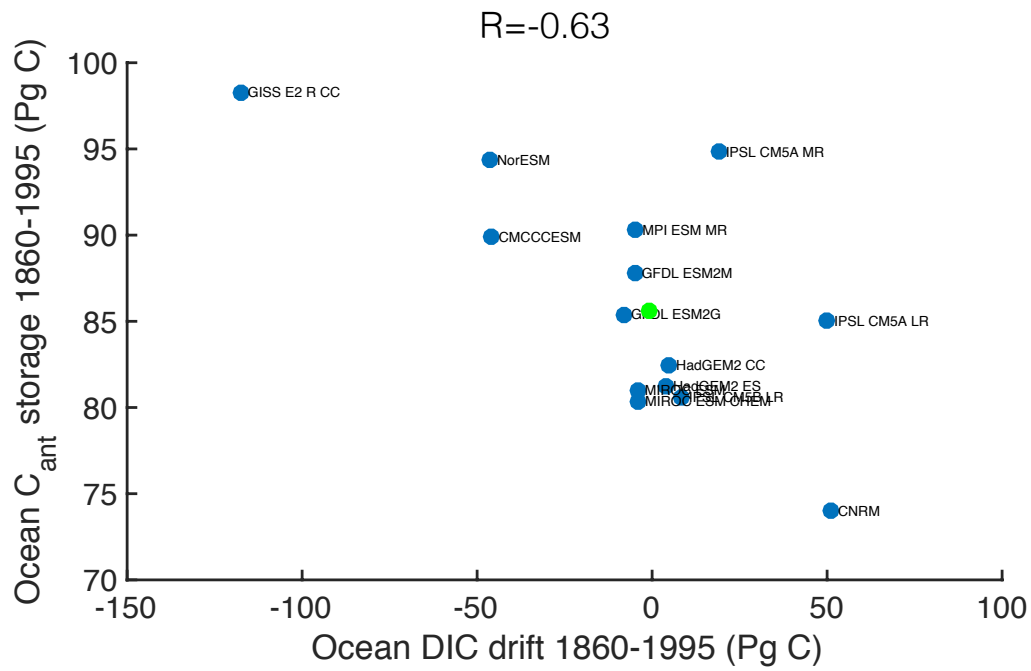
Figure 5. Scatter plot of the drift in oceanic carbon between 1860 and 1995 in the control simulation against the total anthropogenic carbon storage over the same period, with a correlation coefficient of -0.63. The blue circles show individual models and the green circle shows the ensemble mean.